Autonomous vehicle control on lane-free roads: A level-k game approach

Zhaohan Wang[*], Mohsen Ramezani, David Levinson

School of Civil Engineering, The University of Sydney, Australia

Extended abstract submitted for presentation at the 12th Triennial Symposium on Transportation Analysis conference (TRISTAN XII)
June 22-27, 2025, Okinawa, Japan

February 27, 2025

Keywords: Autonomous vehicle, lane-free, receding horizon optimization, game theory

1 INTRODUCTION

Autonomous vehicles (AVs) equipped with advanced sensory systems and efficient actuators offer promising benefits in both travel efficiency and safety. So far, the majority of the research has focused on the development of lane-based control methods, where vehicles travel with lane discipline considerations. Traditionally, in an environment with homogeneous vehicle widths, lanes have improved both the efficiency and safety of human driving by simplifying the driving task to mainly longitudinal car-following maneuvers. Lateral lane-changes are considered more complex and riskier, as drivers need to operate in both longitudinal and lateral directions. AVs, on the other hand, can rely on their efficient sensors and fast reactions to navigate complex two-dimensional planes. AVs open up the potential for a variety of vehicle types and sizes, matched to the specific needs of a particular trip. Recently, there has been increasing interest in the concept of AVs operating on lane-free roads Papageorgiou *et al.* (2021). Unlike traditional roads with designated lanes to guide human drivers, lane-free roads allow AVs to move more flexibly and adaptively. This approach could lead to more efficient use of road space and smoother traffic flow, as AVs optimize their paths without the constraints of fixed lanes.

Both centralized (Levy & Haddad (2021) among others) as well as decentralized (Karafyllis *et al.* (2022) among others) control strategies have been developed for lane-free traffic. The decentralized approach shows promise, especially while the AV penetration rate remains below 100 percent, which is to say, for the foreseeable future. In light of the above viewpoints, this paper presents a decentralized, game-theoretic controller for a lane-free environment.

2 METHODOLOGY

The OCP is defined as a receding horizon control problem with nonlinear costs and dynamics. We define the state vector and the control vector using the kinematic bicycle model. The state vector for a vehicle is defined by four variables ($\mathbf{z(t)} = [x(t), y(t), v(t), \psi(t)]^{\mathrm{T}}$), where $x(t)$ and $y(t)$ denote Cartesian coordinates in the global frame, $v(t)$ is the velocity at the vehicle's center of mass, and $\psi(t)$ indicates the heading in the global frame. The control inputs are expressed as a vector of two variables ($\mathbf{u(t)} = [a(t), \delta(t)]^{\mathrm{T}}$), which correspond to the acceleration $a(t)$ and the front wheel steering angle $\delta(t)$. The kinematics of the vehicle are governed by a set of

[*]Corresponding author.
Email address: zhaohan.wang@sydney.edu.au

nonlinear, coupled ordinary differential equations ($\dot{\mathbf{z}}(t) = \mathbf{f}(\mathbf{z}(t), \mathbf{u}(t))$). A vehicle is characterized by its index, x-position, y-position, velocity, heading, length, and width. These vehicle dynamics and configuration variables are collectively referred to as a vehicle's extended state ($\mathbf{Z}(t) = [id, x(t), y(t), v(t), \psi(t), l, w]^{\mathrm{T}}$), hereinafter referred to as states.

Moreover, the vehicles are subject to the physical limits of their controls, where the admissible control space is defined as a 2-dimensional continuous range with fixed bounds:

$$\mathcal{U} = \{(a(t), \delta(t)) \mid a_{\min} \leq a(t) \leq a_{\max},\ \delta_{\min} \leq \delta(t) \leq \delta_{\max}\}. \tag{1}$$

The optimal control of an ego vehicle ($\mathbf{u}^*(t)$) is obtained by solving the receding horizon optimization problem online. This is done by minimizing the cost function over a prediction horizon subject to the system dynamics constraint, the admissible control constraint, and the collision-avoiding inequality constraint:

$$\text{Minimize: } \mathcal{L}(\mathbf{Z}, \mathbf{u}|t_0) = \int_{t_0}^{t_0+T} g(\mathbf{Z}(t), \mathbf{u}(t))\mathrm{d}t$$

$$\text{subject to: } \begin{cases} \dot{\mathbf{Z}}(t) = \mathbf{f}(\mathbf{Z}(t), \mathbf{u}(t)) & \text{ego vehicle dynamics constraint} \\ \dot{\mathbf{Z}}^{\text{-}}(t) = \mathbf{f}(\mathbf{Z}^{\text{-}}(t), \mathbf{u}^{\text{-}}(t)) & \text{opponent vehicles dynamics constraint} \\ \mathbf{h}(\mathbf{Z}(t), \mathbf{Z}^{\text{-}}(t)) \leq 0 & \text{collision-avoiding constraint} \\ \mathbf{u}(t)\ \ \&\ \ \mathbf{u}^{\text{-}}(t) \in \mathcal{U} & \text{admissible control constraint} \end{cases}$$

where t_0 is the current time, T is the prediction horizon, $\mathcal{L}$ is the cost function, g is the running cost, $\mathbf{h}$ is the inequality constraint, $\mathbf{Z}$ and $\mathbf{u}$ are respectively the state and control vectors of the ego vehicle, and $\mathbf{Z}^{\text{-}}$ and $\mathbf{u}^{\text{-}}$ are the state and control vectors of the opponent vehicles. The OCP is defined with no terminal conditions.

The running cost (g) is defined as a combination of perceived costs. We assume each vehicle has its own preferences regarding the cost components that represent its trade-off between safety and efficiency. However, the overall structure of the cost function is the same for all vehicles.

$$g(\mathbf{Z}(\kappa), \mathbf{u}(\kappa)) = q_1(v_{\text{safe}}(\kappa) - v(\kappa))^2 + q_2\psi(\kappa)^2 + q_3 a(\kappa)^2 + q_4\delta(\kappa)^2 \tag{2}$$

where q_1, q_2, q_3, and q_4 are weights to the cost components. The safe velocity v_{safe} is determined by:

$$v_{\text{safe}}(\kappa) = \min\left(v_{\text{d}}, -\Delta t a_{\min} + \sqrt{\Delta t^2 a_{\min}^2 + v_{\text{p}}(\kappa)^2 + 2a_{\min}(x_{\text{p}}(\kappa) - x(\kappa))}\right) \tag{3}$$

where v_{d} represents the desired velocity, v_{p} is the velocity of the preceding car, and x_{p} is the x-position of the preceding car. The preceding car is defined as the nearest front opponent that overlaps with the ego vehicle when projected onto the front edge of the ego vehicle. The four cost components are, respectively, used to penalize the deviation to the safe speed, vehicle sway, excessive acceleration/braking, and excessive steering.

Vehicles are believed to avoid collisions at all times, whether with the road boundaries or with other vehicles. Therefore, collisions are accounted in inequality constraints defined below:

$$\mathbf{h}(\mathbf{Z}(\kappa), \mathbf{Z}^{\text{-}}(\kappa)) = \begin{bmatrix} -(y(\kappa) - w/2) + \Omega^- \\ (y(\kappa) + w/2) - \Omega^+ \\ -\Delta d_j(\kappa), \quad \forall j \in \mathrm{J}^- \end{bmatrix} \leq 0 \tag{4}$$

where Ω^+ and Ω^- are the upper and lower road bounds, and Δd_j represents the distance between the ego vehicle and the j^{th} opponent in the set of opponents J^-. We assume the vehicle heading is approximately 0 for the road boundary constraints, while this assumption is relaxed for the vehicle collision constraint.

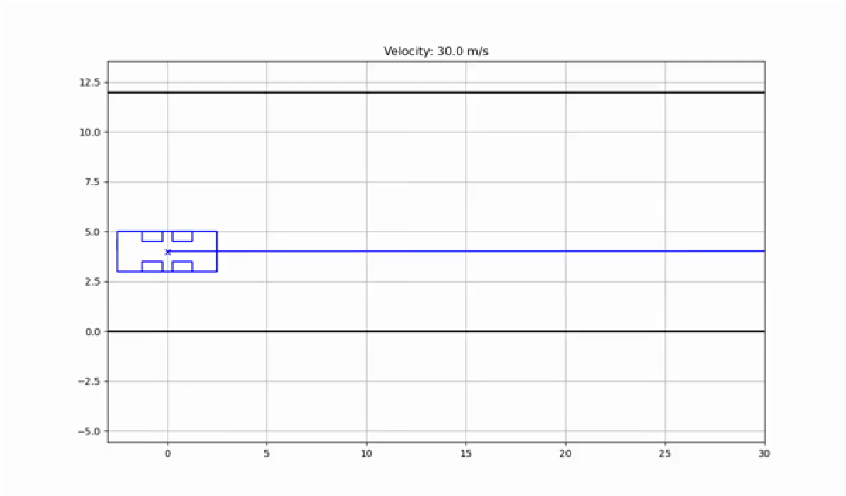

Figure 1 – *Animation of scenario 1. The camera is focused on Vehicle 1.*

To solve the above OCP in real-time, we discretize the horizon into N finite steps and the optimal control is solved online using the continuation/GMRES method, which ensures convergence within a fixed number of iterations Ohtsuka (2004). Since our model involves the prediction of opponents' states and controls over the prediction horizon, we employ level-k game theory to tackle this interaction. For an ego vehicle with a rationality level K, its optimal actions ($\mathbf{u}^{K*}$) can be computed as follows:

$$
\begin{aligned}
\mathbf{u}^{k*} &= \arg\min_{\mathbf{u}^k} \mathcal{L}(\mathbf{Z}^k, \mathbf{u}^k | t_0), \qquad k = 1, 2, ..., K \\
\text{subject to: } & \begin{cases}
\mathbf{Z}^k(\kappa+1) = \mathbf{Z}^k(\kappa) + \mathbf{f}(\mathbf{Z}^k(\kappa), \mathbf{u}^k(\kappa))\Delta t, \qquad k = 1, 2, ..., K \\
\mathbf{Z}^{k-1}(\kappa+1) = \mathbf{Z}^{k-1}(\kappa) + \mathbf{f}(\mathbf{Z}^{k-1}(\kappa), \mathbf{u}^{k-1}(\kappa))\Delta t, \qquad k = 1, 2, ..., K \\
\mathbf{h}(\mathbf{Z}^k(\kappa), \mathbf{Z}^{k-1}(\kappa)) \leq 0, \qquad \forall \kappa \in 0, ..., N-1, \qquad k = 1, 2, ..., K \\
\mathbf{u}^k(\kappa) \;\&\; \mathbf{u}^{k-1}(\kappa) \in \mathcal{U}, \qquad \forall \kappa \in 0, ..., N-1, \qquad k = 1, 2, ..., K
\end{cases}
\end{aligned}
$$

where $\mathbf{Z}^k$ denotes the states of level k vehicles, $\mathbf{u}^k$ denotes the actions adopted by the level k vehicles, and $\mathbf{u}^{0*} = \mathbf{0}$. The level 0 cars in this study are assumed to travel at constant velocities, where the acceleration and steering are both zero. Since we are experimenting on a small fleet, the opponents of an ego vehicle are identified as all other vehicles in the fleet.

3 SIMULATION RESULTS

The above control framework is tested using two simulation scenarios. The first simulation scenario involves four vehicles positioned sparsely apart. The simulation results for scenario 1 are shown in an animation in Figure 1 (Please download the pdf to watch it in Acrobat Reader). It can be seen that all vehicles avoid collisions with each other and with road boundaries at all times. When vehicles come close, they avoid each other by moving in opposite directions laterally. Vehicles converge to their desired velocities in a short period of time when no preceding vehicles are detected. When there are preceding cars, vehicles behave in a car-following manner by reducing their speeds. Vehicles also tend to move towards the centre of the road over time, which might be due to the road bound constraints. This ensures vehicles have enough room to operate laterally.

The second set of simulations is conducted on closely initialized vehicles. The simulated states over a length of 30 seconds are shown in an animation in Figure 2 (Please download the

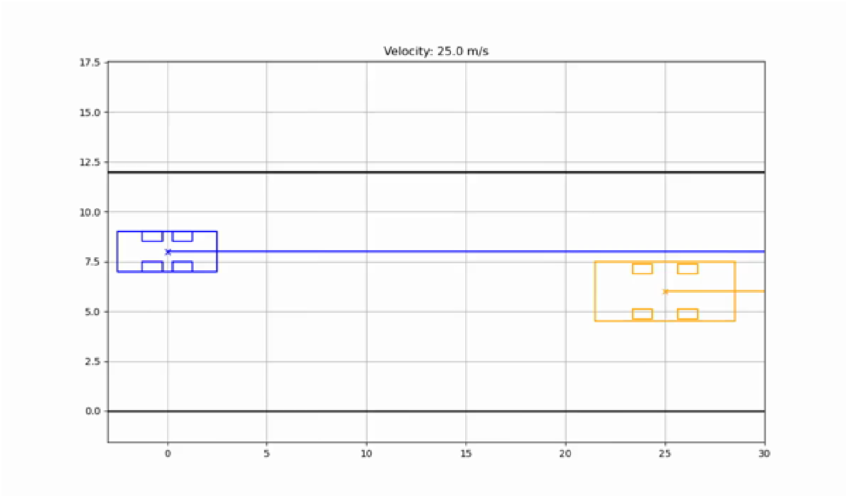

Figure 2 – *Animation of scenario 2. The camera is focused on Vehicle 1. Click to watch again.*

pdf to watch it in Acrobat Reader). Once again, it can be observed that vehicles avoid each other as they come close due to the effect of the collision-avoidance constraint. Between 5-15 seconds in the simulation, Vehicles 3, 2, and 1 have bypassed the slower Vehicle 4 by moving laterally towards the right. Vehicle 4 also moves to the left to make space for the other vehicles. Vehicle 1 then bypasses Vehicle 2 at approximately 25 seconds. It is clear from the velocity-time plot that vehicles can converge to their desired velocities. When there are preceding cars in front, the vehicle tends to reduce its velocity, then gradually increases speed again after overtaking. This is most apparent in Vehicle 1 as it maintains a safe distance from its preceding cars and finally reaches its desired velocity towards the end of the simulation.

4 DISCUSSION

Future research should expand the testing scenarios. For instance, we are in process of testing performance with significantly more vehicles in the fleet and designing more efficient opponent identification heuristics. Additional research should test with a heterogeneous vehicle fleet of varying compositions, with vehicles of different lengths and widths (as tested here) as well as heights (visual range, blockage of other vehicle's visual range) and masses (which affects braking distance and cost of collision should one occur), thus better representing small and large cars, small and large trucks, three-wheelers, and motorcycles. These results should be compared with lane-based traffic regulation for understanding of the trade-offs of vehicle throughput and safety under different fleet compositions.

References

Karafyllis, Iasson, Theodosis, Dionysios, & Papageorgiou, Markos. 2022. Lyapunov-based two-dimensional cruise control of autonomous vehicles on lane-free roads. *Automatica*, **145**(Nov.), 110517.

Levy, Rotem, & Haddad, Jack. 2021. Path and Trajectory Planning for Autonomous Vehicles on Roads without Lanes. *Pages 3871–3876 of: 2021 IEEE International Intelligent Transportation Systems Conference (ITSC)*. Indianapolis, IN, USA: IEEE.

Ohtsuka, Toshiyuki. 2004. A Continuation/GMRES Method for Fast Computation of Nonlinear Receding Horizon Control. *Automatica*, **40**(4), 563–574.

Papageorgiou, Markos, Mountakis, Kyriakos-Simon, Karafyllis, Iasson, Papamichail, Ioannis, & Wang, Yibing. 2021. Lane-Free Artificial-Fluid Concept for Vehicular Traffic. *Proceedings of the IEEE*, **109**(2), 114–121.